Chaos, Solitons and Fractals 103 (2017) 294–306

Contents lists available at ScienceDirect

Chaos, Solitons and Fractals

Nonlinear Science, and Nonequilibrium and Complex Phenomena

journal homepage: www.elsevier.com/locate/chaos

Volumetric behavior quantification to characterize trajectory in phase space

Hamid Niknazar[a], Ali Motie Nasrabadi[b,*], Mohammad Bagher Shamsollahi[c]

[a] Department of Biomedical Engineering, Science and Research Branch, Islamic Azad University, Tehran, Iran
[b] Department of Biomedical Engineering, Shahed University, Tehran, Iran
[c] Bimedical Signal and Image Processing lab, School of Electrical Engineering, Sharif University of Technology, Tehran, Iran

ARTICLE INFO

Article history:
Received 10 January 2017
Revised 29 May 2017
Accepted 18 June 2017

Keywords:
Nonlinear quantifier
Volumetric behavior
Phase space
Complexity

ABSTRACT

This paper presents a methodology to extract a number of quantifier features to characterize volumetric behavior of trajectories in phase space. These features quantify expanding and contracting behaviors and complexity that can be used in nonlinear and chaotic signals classification or clustering problems. One of the features is directly extracted from the distance matrix and seven features are extracted from a matrix that is subsequently obtained from the distance matrix. To illustrate the proposed quantifiers, Mackey–Glass time series and Lorenz system were employed and feature evaluation was performed. It is shown that the proposed quantifier features are robust to different initializations and can quantify volumetric behavior characteristics. In addition, the ability of these features to differentiate between signals with different parameters is compared with some common nonlinear features such as fractal dimensions and recurrence quantification analysis features.

1. Introduction

There are two separate, but interacting lines of development characterizing chaos and nonlinear theory. The first line focuses on ordinary nonlinear differences and differential equations that may have chaotic behavior meaning the system is available. In the second line, the system is not available and relies heavily on the computational study of chaotic system outputs and includes methods for investigating potential chaotic behavior in observed time series.

Describing global and local behavior of trajectories can lead to a better understanding of attractor properties. These properties of attractor can give us valuable information about systems and their behavior. For example, Lyapunov exponents that are extracted from trajectory can indicate dissipation of the system [1]. In this paper, eight features based on local and global behaviors of trajectory in phase space are proposed in terms of volumetric and complexity. Lyapunov exponents provide rate of local separation in each dimension of space, while the proposed method can provide a single value of expansion rate for the whole trajectory globally. Moreover, the rates of expansion and contraction will be achieved separately. Fractal dimensions focus on occupying space capacity in detail [2], whereas the proposed method presents a feature that provides occupied space globally. The complexity feature in the proposed method presents a new meaning of complexity that has a different meaning from approximate [3] and sample [4] entropies. This meaning has a relationship with the variations in expansion and contraction speed. Some of the proposed features have independent meanings and some other features have meanings in comparison to other features. These features quantify some properties of the trajectories obtained from nonlinear and chaotic signals. Therefore, they can be employed in classification problems in applications such as biomedical signal processing, finance, electronics, etc, in which the observed signals are nonlinear or chaotic.

The rest of the paper is organized as follows. Section 2 reviews some related works. The proposed method is described in Section 3. Section 4 is devoted to evaluate and discuss the proposed method by comparing two nonlinear systems with different parameters. Finally, our conclusions are stated in Section 5.

2. Related work

In many studies, trajectory in phase space is reconstructed from time series and features or properties are extracted. These features characterize the behavior of trajectories or attractors that help to identify or classify systems and trace their changes. For example,

* Corresponding author.
E-mail addresses: hd.niknazar@gmail.com (H. Niknazar), nasrabadi@shahed.ac.ir (A.M. Nasrabadi), mbshams@sharif.edu (M.B. Shamsollahi).

http://dx.doi.org/10.1016/j.chaos.2017.06.018
0960-0779/

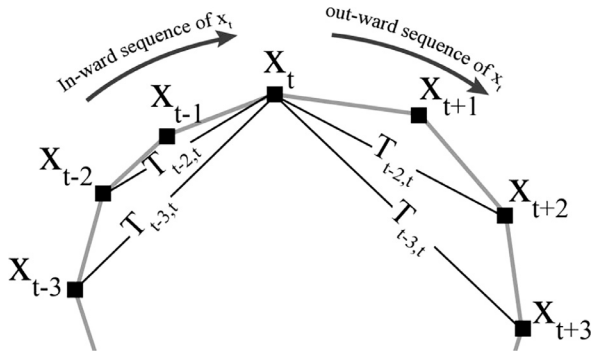

Fig. 1. Trajectory in phase space. In-ward and out-ward sequences of $\mathbf{x}_t$ are shown. $\mathbf{T}_{i,j}$ is distance between $\mathbf{x}_i$ and $\mathbf{x}_j$.

there are entropy-based features [5] such as approximate entropy (ApEn) [3], which is a technique to quantify the amount of regularity and unpredictability of fluctuations over time-series data [6], and sample entropy (SampEn), which is a modification of approximate entropy, used extensively for assessing complexity of a physiological time-series signal, thereby diagnosing diseased state [4]. Lyapunov exponent is a quantifier that characterizes the rate of separation of infinitesimally close trajectories [1,7]. The characteristics of some features are focused on measuring the space-filling capacity of patterns that illustrate how a fractal scales differently from the space it is embedded in [8], namely Fractal dimension [2] such as Higuchi [9]. Katz feature [10] characterizes stretching and distribution of trajectory in phase space by comparing the relationship between the length of trajectory and diagonals. In some cases, quantification of behavior of signals or systems is done by a transform such as Discrete Fourier Transform (DTF) [11], Discrete Wavelet Transform(DWT) [12], and Singular Value Decomposition (SVD) [13]. These transforms are relatively general and can be used in a variety of applications. Local Fractional z-Transforms [14], Local Fractional Continuous Wavelet Transform [15] and Local Fractional Discrete Wavelet Transform [16] are examples of more specific transforms applied on signals that are defined on cantor sets. Recurrence quantification analysis (RQA) [17] characterizes recurrence and returning behavior of a trajectory by using Recurrence Plot (RP) [18]. All of these features characterize properties of behavior of trajectories in phase space and each is used in many applications in physics, finance or engineering [19–26].

3. Method

This paper proposes a method to extract features from phase space of nonlinear systems. In this study, we focus on finding properties of trajectories that can present "volumetric behavior" of sequence of state vectors. Volumetric behavior characterizes occupied space and changes in occupied space of trajectory in space. First, we introduce the concept of phase space availability Section 2.1), and then we present a method to extract appropriate features (Section 2.2). This section is followed by describing these features (Section 2.3).

3.1. Trajectories in phase space

Dynamical systems are usually represented in three types: 1- phase space 2- time series 3- time-evolution law. In a d-dimensional phase space of a dynamic system at a fixed time t, the state of the system can be specified by d variables. These variables form vector $\vec{\mathbf{x}}(t)$:

$$\vec{\mathbf{x}}(t) = (x_1(t), x_2(t), \ldots, x_d(t))^T \tag{1}$$

For continuous-time systems, the evolution time is given by a set of differential equations. In fact, the evolution time law allows us to determine the state of the system at time t from the state at all previous times.

$$\vec{\mathbf{x}}\cdot(t) = \frac{d(\vec{\mathbf{x}}(t))}{dt} = F(\vec{\mathbf{x}}), \qquad F : R^d \rightsquigarrow R^d \tag{2}$$

The vector $\vec{x}(t)$ defines a trajectory in d-dimensional phase space.

In an experimental setting, we do not often have access to all d states of phase space and a single discrete time measurement is available. In this case, phase space has to be reconstructed from time series $x(t) = \{x_1, x_2, ?, x_N\}$ [27]. Takens method [28] is frequently used for reconstructing phase space from time series $x(t)$ using two parameters embedding dimension μ and delay τ:

$$\vec{\mathbf{x}}_i(t) = (x_i, x_{i+\tau}, \ldots, x_{i+(\mu-1)\tau}), \qquad i = [1 \quad N-(\mu-1)\tau] \tag{3}$$

The false nearest-neighbors algorithm [29] and the mutual information [30] can be used for choosing appropriate dimension μ and delay τ parameters, respectively.

In next subsection, we propose a method to quantify volumetric behavior of trajectory.

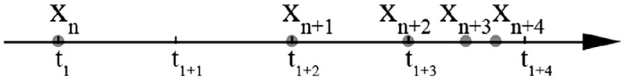

$$T = \begin{pmatrix} 0 & 2 & 3 & 3.5 & 3.75 \\ 2 & 0 & 1 & 1.5 & 1.75 \\ 3 & 1 & 0 & 0.5 & 0.75 \\ 3.5 & 1.5 & 0.5 & 0 & 0.25 \\ 3.75 & 1.75 & 0.75 & 0.25 & 0 \end{pmatrix} \rightarrow T_1 = \begin{pmatrix} 2 & 3 & 3.5 & 3.75 \\ 2 & 1 & 1.5 & 1.75 \\ 3 & 1 & 0.5 & 0.75 \\ 3.5 & 1.5 & 0.5 & 0.25 \\ 3.75 & 1.75 & 0.75 & 0.25 \end{pmatrix}$$

$$\rightarrow T^* = \begin{pmatrix} -1 & -0.5 & -0.25 \\ 1 & -0.5 & -0.25 \\ 2 & 0.5 & -0.25 \\ 2 & 1 & 0.25 \\ 2 & 1 & 0.5 \end{pmatrix}$$

Fig. 2. An example of calculating matrix $\mathbf{T}^*$. x_n, x_{n+1}, x_{n+2}, x_{n+3} and x_{n+4} are stated in one-dimensional space. $\mathbf{T}$ is distance matrix that is provided by calculating distance of each pair of states. Matrix $\mathbf{T_1}$ is achieved by removing the main diagonal of matrix T. This matrix is converted to $\mathbf{T}^*$ by using Eq. (8).

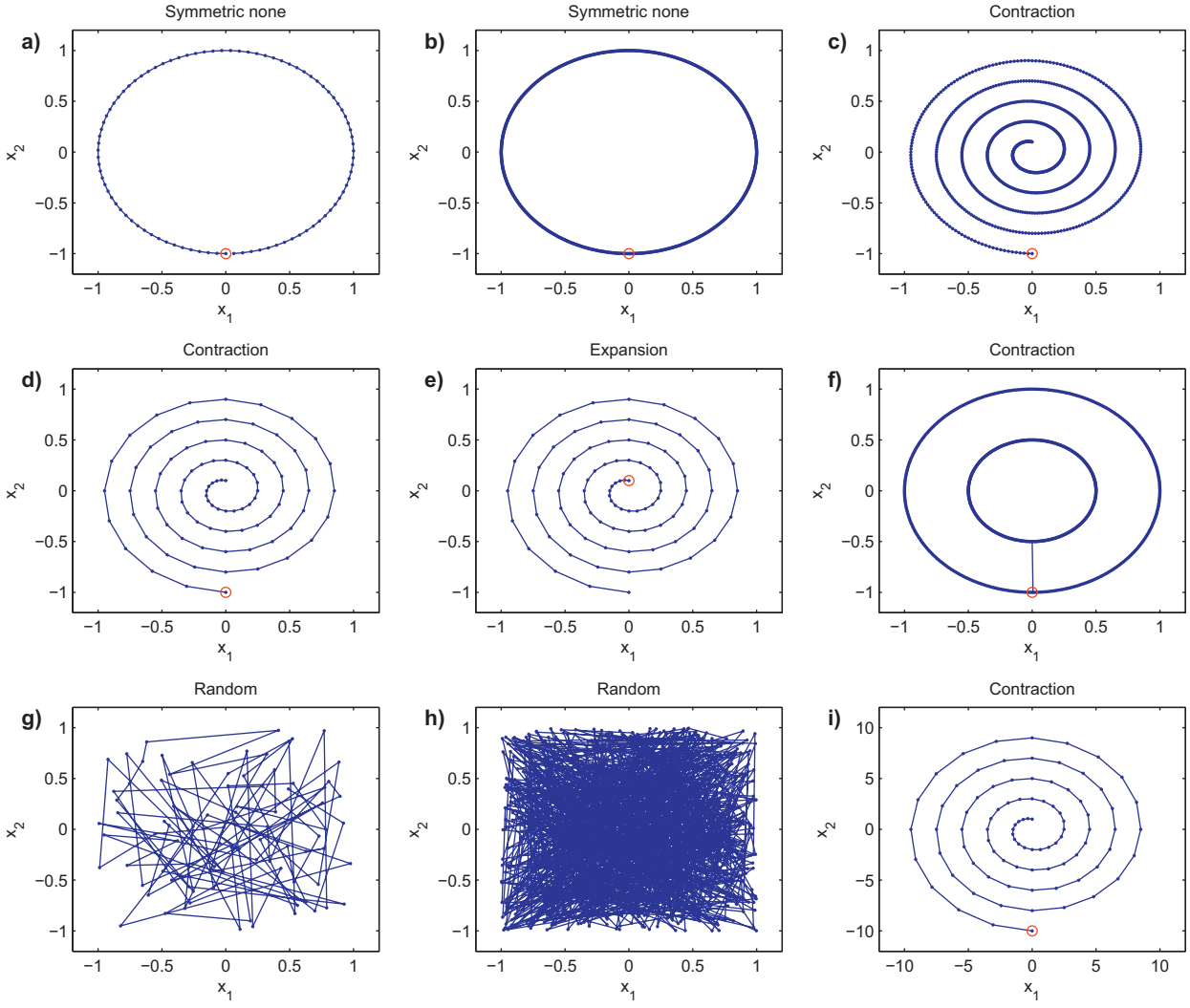

Fig. 3. Samples of different volumetric behavior of trajectory in phase space. Red circle is start time.

3.2. Volumetric behavior of trajectory

The proposed method is based on volumetric behavior of trajectory and extracts features that can reveal a number of characteristics of trajectory in phase space.

3.2.1. Definitions

Suppose trajectory L is constructed from N state vectors:

$$L = \vec{\mathbf{x}}_1, \vec{\mathbf{x}}_2, \ldots, \vec{\mathbf{x}}_N. \tag{4}$$

Before extracting features, we need to define matrix **T** and **T*** which include information about the relationship between state vectors. Distance matrix **T** is given by Eq. (5) which presents distance between all vector states of trajectory:

$$\mathbf{T_{i,j}} = Distance(\vec{\mathbf{x}}_i, \vec{\mathbf{x}}_j), \qquad i, j = [1 \quad N]$$

$$\mathbf{T} = \begin{bmatrix} 0 & T_{1,2} & \ldots & T_{1,N} \\ T_{2,1} & 0 & \ldots & T_{2,N} \\ \vdots & \vdots & \ddots & \vdots \\ T_{N,1} & \ldots & \ldots & 0 \end{bmatrix} \tag{5}$$

Matrix T is the basis of recurrence plots method [17]. Recurrence plots method uses the Heaviside function Θ(x)and matrix $R_{i,j}$ is obtained as:

$$R_{i,j}(\varepsilon) = \Theta(\varepsilon - \mathbf{T}_{i,j}), \qquad i, j = [1 \quad N] \tag{6}$$

where ε is distance threshold.

Matrix **T** is the source of "Occupied Space (OS)" feature that is described in Section 2.2.2 and used to construct matrix **T***. Before this construction, three definitions are needed:

- Moving forward through time: sequence of occurrence times of state vector. As in Fig. 1, order of state vectors in time is displayed by subscripts.
- In-ward and out-ward sequences of state vector $\vec{\mathbf{x}}_t$: if by moving forward through time, subscript of state vector gets closer to t, we have an in-ward sequence of state vector $\vec{\mathbf{x}}_t$. Conversely, if by moving forward through time, subscript of state vectors gets away from t, we have an out-ward sequence of state vector $\vec{\mathbf{x}}_t$ (Fig 1). For example, sequence { $\vec{\mathbf{x}}_{t-2}$, $\vec{\mathbf{x}}_{t-1}$, $\vec{\mathbf{x}}_t$ } is an in-ward sequence and sequence { $\vec{\mathbf{x}}_t$, $\vec{\mathbf{x}}_{t+1}$, $\vec{\mathbf{x}}_{t+2}$ } is an out-ward sequence.
- Getting closer to (or getting away from) the state vector $\vec{\mathbf{x}}_t$: in an out-ward sequence of state vector if moving forward through time, (or in an in-ward sequence moving backward through time,) causes reduction (or increase) of distance between state vectors and state vector $\vec{\mathbf{x}}_t$ (T in Fig. 1) we have getting closer to (or away from) the state vector $\vec{\mathbf{x}}_t$.

In the proposed method in Section 2.2.2, eight features will be presented to characterize global behavior of getting closer to and away from state vectors that is the meaning of volumetric behav-

Table 1
Value of eight features of the method that are extracted from Fig. 3 trajectories.

	no. states	OS	ACS	AES	AC	AE	SDCS	SDES	Complexity
a	90	1.27311	0.03374	0.03378	0.01687	0.01687	0.01692	0.01689	0.01691
b	900	1.27324	0.00348	0.00348	0.00174	0.00174	0.00169	0.00169	0.00169
c	900	0.76973	0.01074	0.01027	0.00565	0.00487	0.00805	0.00800	0.00803
d	90	0.77053	0.1037	0.09849	0.05452	0.04671	0.07772	0.07716	0.07745
e	90	0.77053	0.09849	0.1037	0.04671	0.05452	0.07716	0.07772	0.07745
f	900	1.00923	0.00623	0.00554	0.00312	0.00277	0.01783	0.00531	0.01158
g	90	1.04832	0.51986	0.54121	0.26272	0.2677	0.36711	0.36354	0.36535
h	900	1.05748	0.51099	0.50583	0.25433	0.25407	0.37294	0.37351	0.37323
i	90	7.70528	0.10370	0.09849	0.05452	0.04671	0.07772	0.07716	0.07745

Table 2
Value of eight features of the method that are extracted from Fig. 4 trajectories.

	no. states	OS	ACS	AES	AC	AE	SDCS	SDES	Complexity
a	50	≈ 0	2.01288	2.01288	0.47722	0.47387	≈ 0	≈ 0	≈ 0
b	50	0.3332	0.05942	0.05942	0.02941	0.02941	0.006	0.006	0.006
c	50	0.33986	0.04041	0.07661	0.01980	0.03907	0.02691	0.03034	0.02866
d	50	0.5000	2	2	0.98	0.98	0	0	0
e	50	0.35316	0.81154	0.84567	0.42132	0.40663	0.61938	0.6384	0.628535

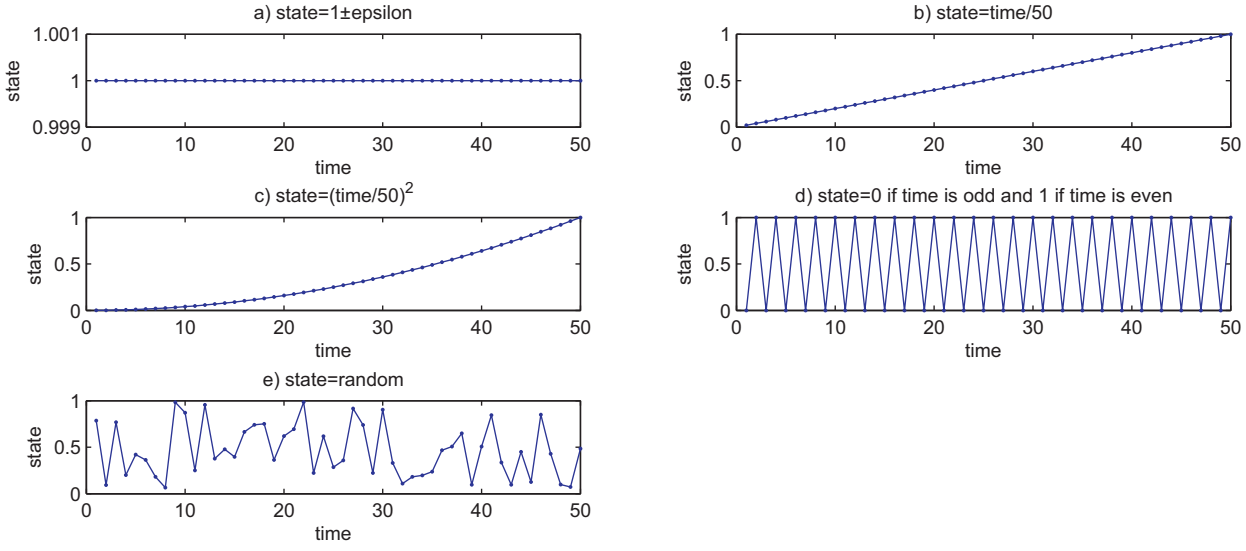

Fig. 4. Samples of different volumetric behavior of trajectory in one-dimensional phase space.

ior. To extract these features, matrix **T*** is defined. Matrix **T*** is constructed from **T** in two steps: in the first step, the elements above the main diagonal are shifted to left and matrix $\mathbf{T_1}$ of size $N*(N-1)$ is built. This is because of removing zero elements of the main diagonal (Eq. (7)).

$$\mathbf{T}_1 = \begin{bmatrix} T_{1,2} & \cdots & T_{1,(N-1)} & T_{1,N} \\ T_{2,1} & \ddots & \cdots & T_{2,N} \\ \vdots & \ddots & \vdots & \vdots \\ T_{(N-1),1} & \cdots & \cdots & T_{(N-1),N} \\ T_{N,1} & \cdots & \cdots & T_{N,(N-1)} \end{bmatrix} \tag{7}$$

In the next step, by using Eq. (8) matrix **T*** is achieved. Each row of this matrix represents distance difference between a state point and other consecutive state points, so by extracting statistical characteristics of matrix **T*** volumetric behavior can be presented. Row j of matrix **T*** represents distance difference between each two sequential state vectors and jth state vector of trajectory. If $i \le j+1$ in $\mathbf{T}_1(i,j)^*$ sequence of difference follows "getting closer to the state vector" and if $i > j+1$ sequence of difference follows "getting away to the state vector".

$$\mathbf{T}^*_{i,j} = \mathbf{T}_{1_{i,j}} - \mathbf{T}_{1_{i,j+1}}, \qquad i = [1 \quad N], \qquad j = [1 \quad N-2] \tag{8}$$

Fig. 2 shows an example of two steps of constructing **T*** matrix from a one-dimensional trajectory. In the next sub-section by using matrix **T** and **T***, eight features will be extracted to characterize volumetric behavior of trajectory.

3.2.2. Extracting features from matrix **T** *and* **T***

Elements of matrix **T** contain information about distance of state vectors. Average of $T_{i,j}$ can be used to characterize occupied space by trajectory. Thus, "occupied space (OS)" feature is defined as Eq. (9):

$$OS = \frac{1}{N^2}\sum_{i=1}^{N}\sum_{j=1}^{N}\mathbf{T}_{i,j} \tag{9}$$

Also **T*** contains information about the behavior of trajectory. Row i of matrix **T*** is arised from the relationship between all state vectors and vector i and is constructed from some positive and negative numbers. Positive numbers are arised from the sequence of $\mathbf{T}_{i,j} - \mathbf{T}_{i,j+1}$ where $\mathbf{T}_{i,j} > T_{i,j+1}$, so in this sequence, trajectory is

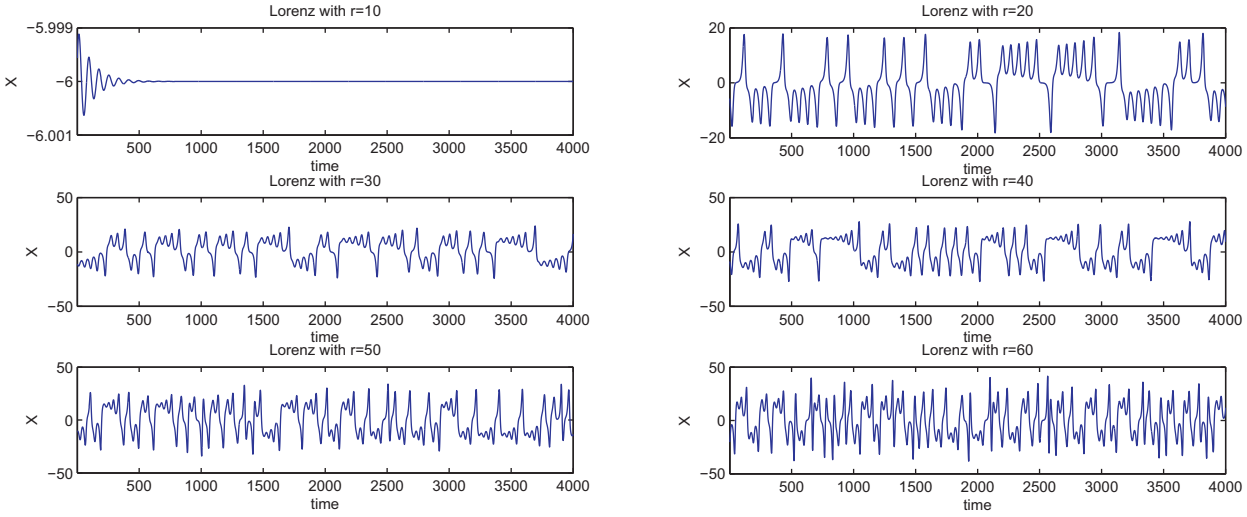

Fig. 5. *X* time series of Lorenz model with different parameters.

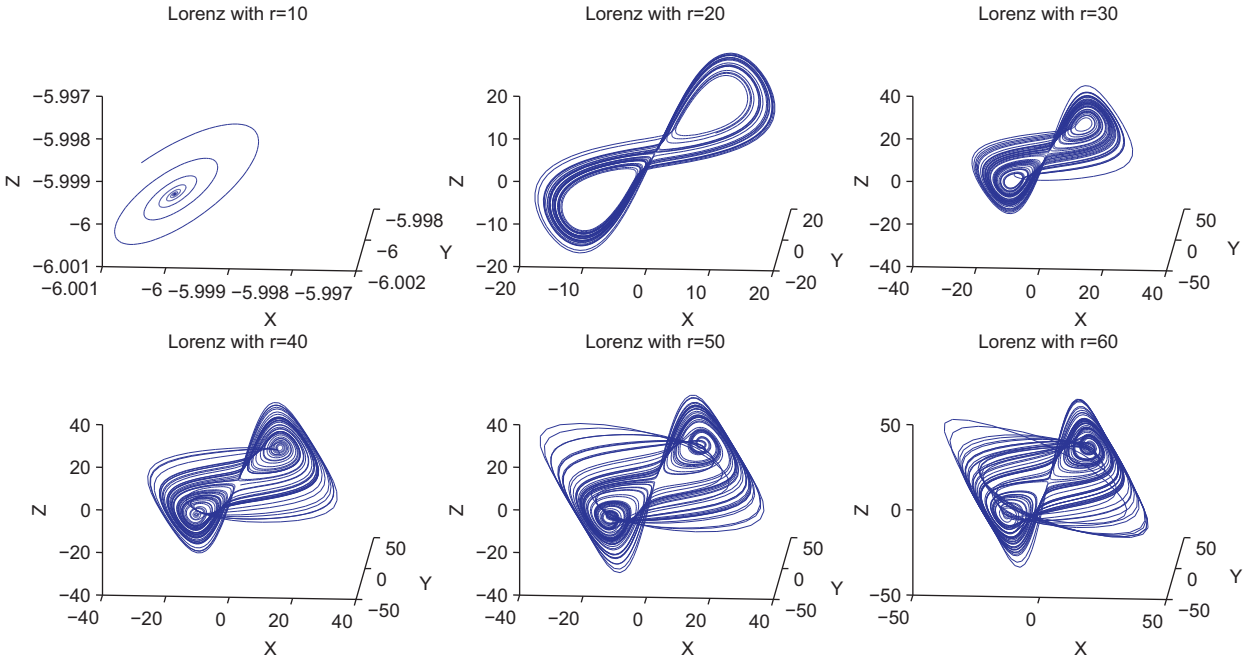

Fig. 6. Embedded trajectories in phase space that are extracted from X time series of Lorenz model with different parameters.

getting closer to $\mathbf{x}_i$ state vector. Conversely, negative numbers are arised from $\mathbf{T}_{i,j} < \mathbf{T}_{i,j+1}$ and in this sequence, trajectory is going away from $\mathbf{x}_i$ state vector. Average value of the positive (or negative) numbers characterizes average speed of trajectory contraction (or expansion) toward $\mathbf{x}_i$ state vector. Therefore, two features "average of expanding speed (AES)" and "average of contracting speed (ACS)" are defined as follows:

$$ACS = \frac{|\frac{1}{p}\sum_{i,j}\ \mathbf{T}^*|}{OS} \qquad (i,j|\mathbf{T}^*_{i,j} > 0),\ (p\text{=number of positive } \mathbf{T}^*_{i,j}) \quad (10)$$

$$AES = \frac{|\frac{1}{n}\sum_{i,j}\ \mathbf{T}^*|}{OS} \qquad (i,j|\mathbf{T}^*_{i,j} < 0),\ (n\text{=number of negative } \mathbf{T}^*_{i,j}) \quad (11)$$

To present expanding or contracting behavior of trajectory, two features of average expanding "AE" and average contracting "AC" are defined as Eqs. (12) and (13), respectively:

$$AC = \frac{|\frac{1}{N*(N-2)}\sum_{i,j}\ \mathbf{T}^*|}{OS} \qquad (i,j|\mathbf{T}^*_{i,j} > 0) \quad (12)$$

$$AE = \frac{|\frac{1}{N*(N-2)}\sum_{i,j}\ \mathbf{T}^*|}{OS} \qquad (i,j|\mathbf{T}^*_{i,j} < 0) \quad (13)$$

Variation of positive and negative numbers of matrix $\mathbf{T}^*$ can characterize volume behavior variation of trajectory. Hence, "standard deviation of expanding speed (SDES)" and "standard deviation of contracting speed (SDCS)" features are defined as Eqs. (14) and (15):

$$SDCS = \frac{std(\mathbf{T}^*_{i,j})}{OS} \qquad (i,j|\mathbf{T}^*_{i,j} > 0) \quad (14)$$

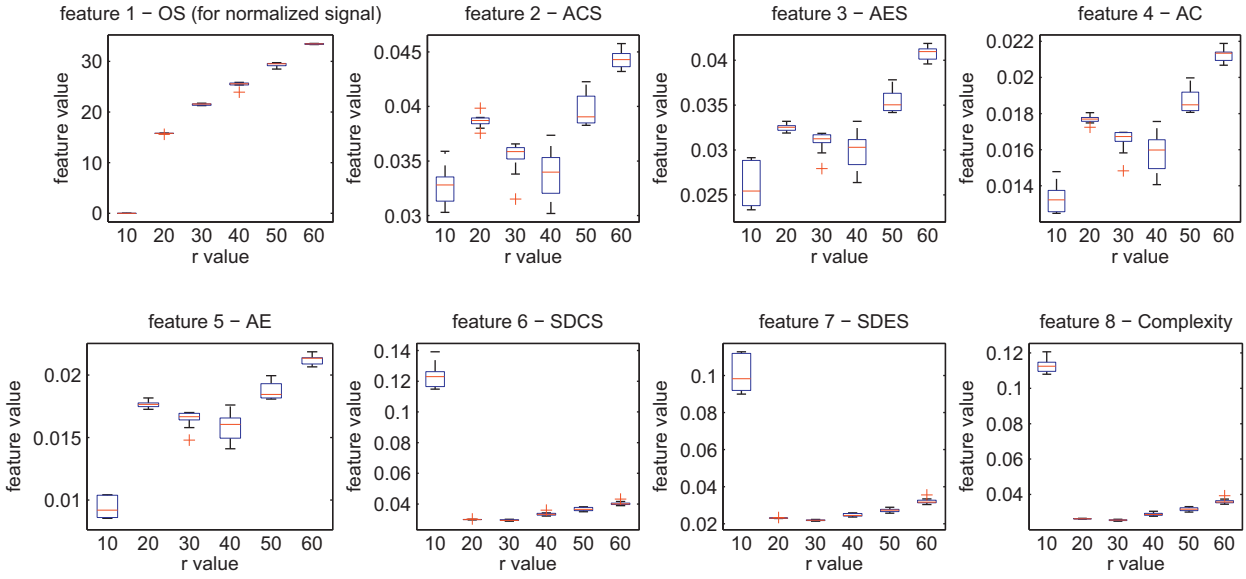

Fig. 7. Box plot of the eight features of the proposed method that are extracted from trajectories of Lorenz model with ten different random initializations.

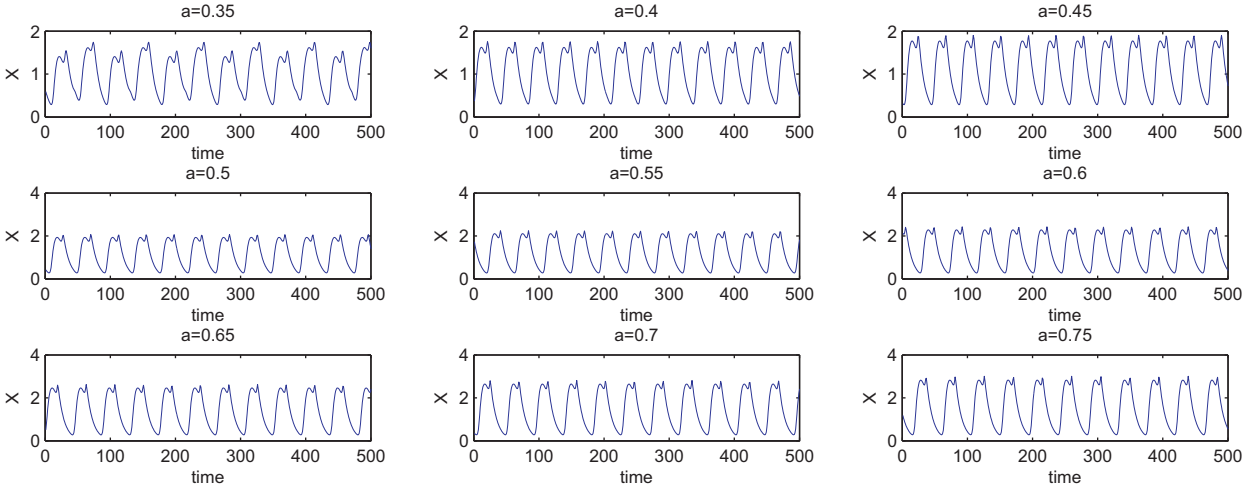

Fig. 8. Time series of Mackey–Glass model with different parameters.

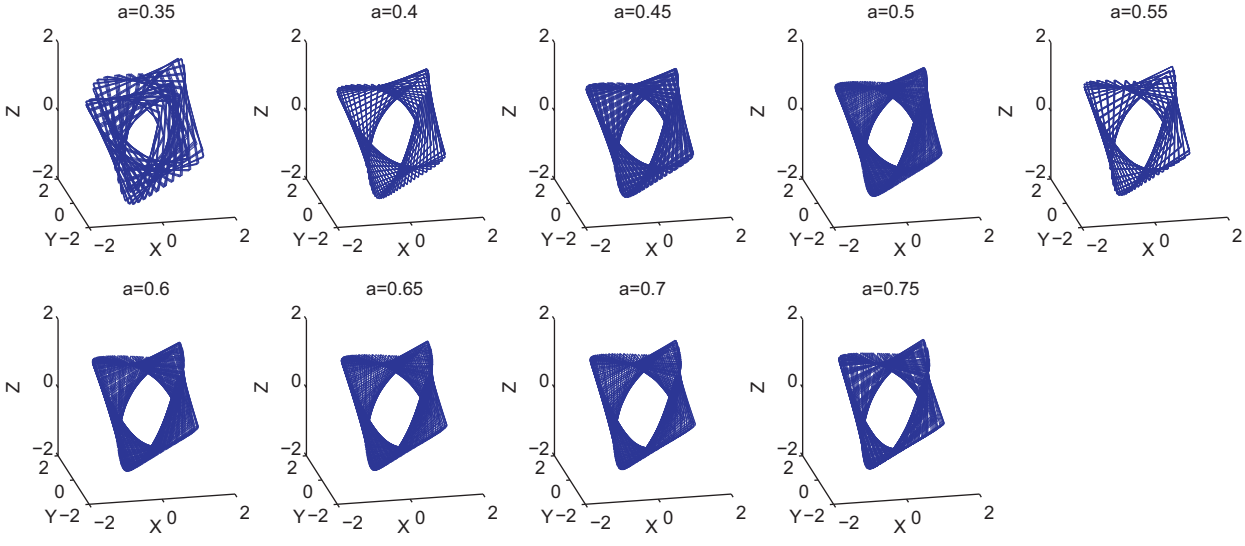

Fig. 9. Embedded trajectories in phase space that are extracted from time series of Mackey–Glass model with different parameters.

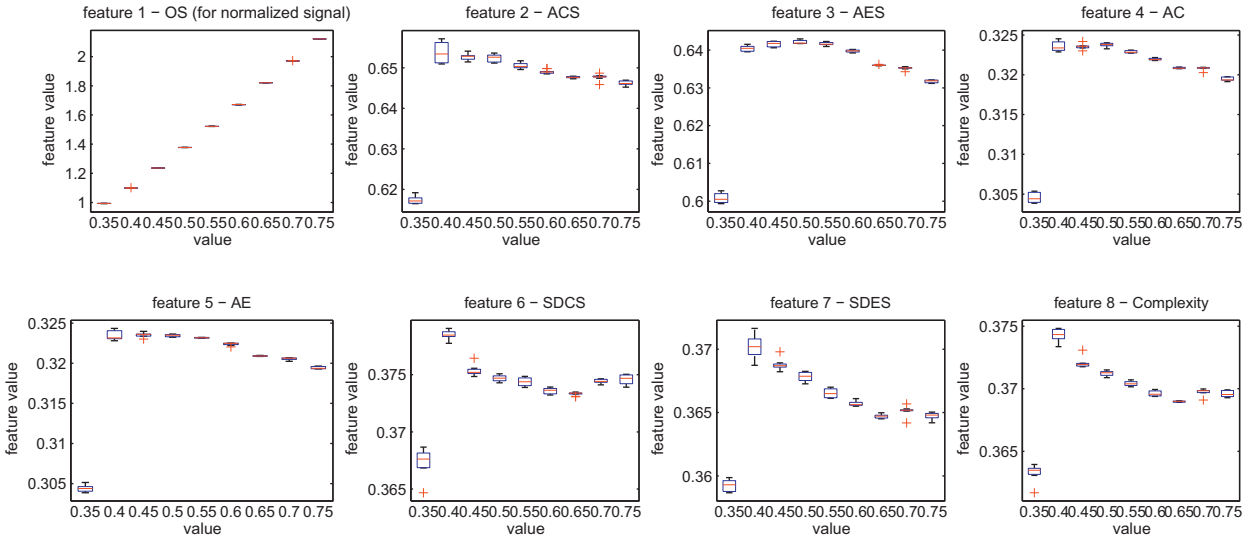

Fig. 10. Box plot of the eight features of the proposed method that are extracted from trajectories of Mackey–Glass model with ten time random initialization.

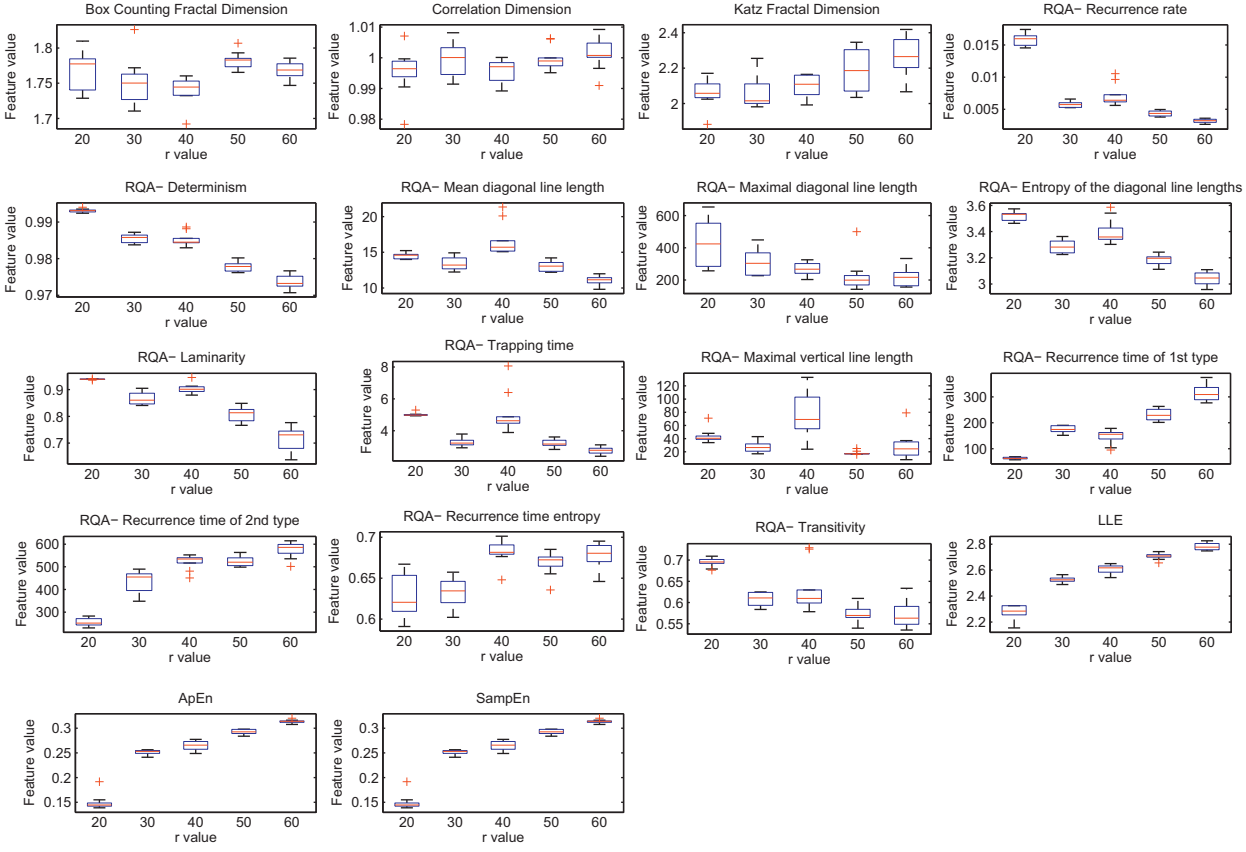

Fig. 11. Box plot of some common nonlinear features: fractal dimensions, RQA features, Largest Lyapunov Exponent (LLE), Approximate and Sample entropy for Lorenz signal with different parameters and random initial points.

$$SDES = \frac{std(\mathbf{T}^*_{i,j})}{OS} \qquad (i, j|\mathbf{T}^*_{i,j} < 0) \tag{15}$$

where $std(x)$ is standard deviation of x.

Each of SDES and SDCS features is limited to either expanding or contracting behavior separately. By mixing these features, Complexity feature is achieved:

$$Complexity = \frac{SDCS * p + SDES * n}{N * (N-2)} \tag{16}$$

3.3. Feature description and discussion

With $d+1$ state vectors in a d-dimensional space, topology (except position and orientation) is achievable by having the distance between these vectors, matrix **T**. On this basis, "occupied space (OS)" feature is defined. This feature characterizes occupied spaces by state vectors independent of time or sequence of state vectors. The value of OS feature depends on the number of state vectors and distance between state vectors but in two trajectories with the

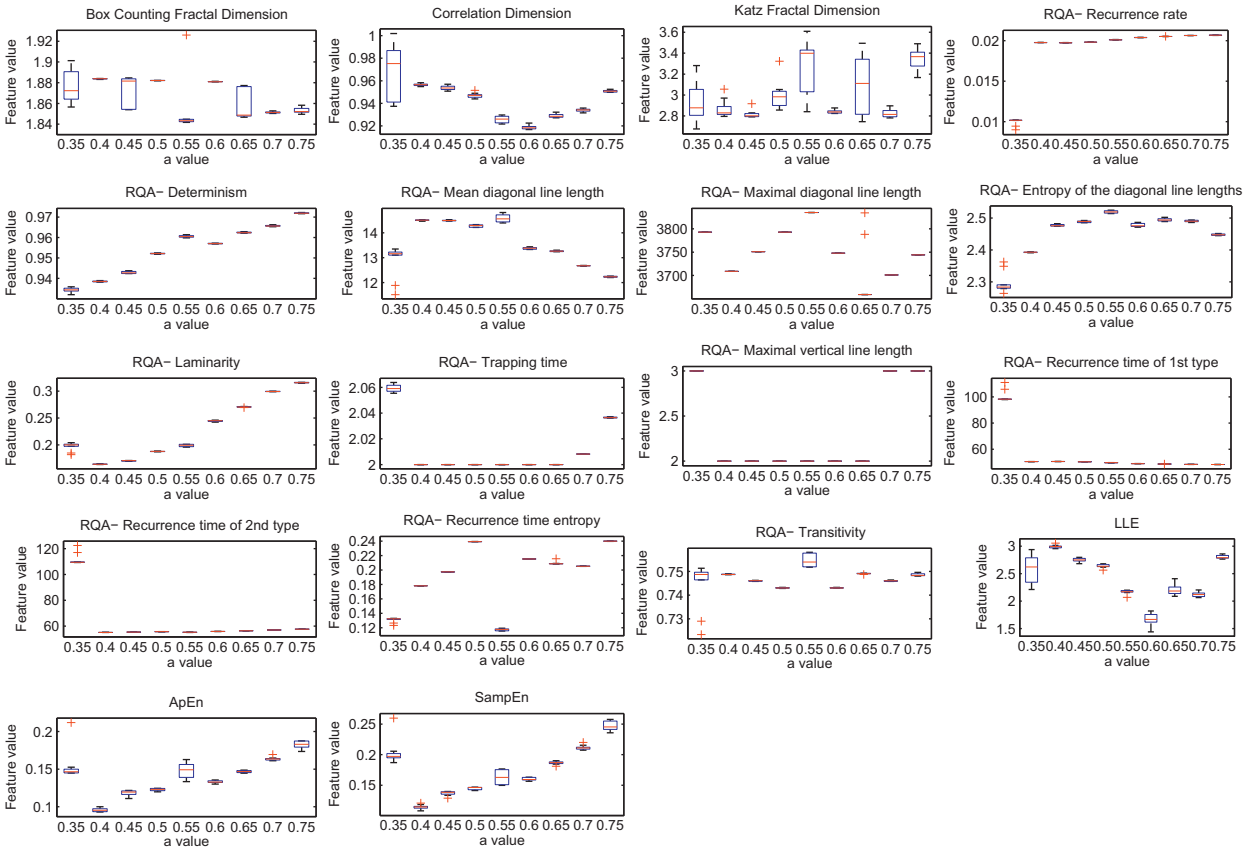

Fig. 12. Box plot of some common nonlinear features: fractal dimensions, RQA features, LLE, Approximate and Sample entropy for Mackey–Glass signal with different parameters and random initial points.

same topology and different numbers of state vectors. OS feature value of these two trajectories is almost the same (Fig. 3a and b). In the same population of state vectors in a d-dimensional convex volume, if points are located on convex volume, OS has maximum value in this d-dimensional convex volume (Fig. 3b OS has greater value compared with that of Fig. 3f).

"AES" against "ACS", "AE" against "AC" and "SDES" against "SDCS" features have dualistic relationships. AES and ACE describe average speed of expanding and contracting. Normalization of these features to the number of positive and negative elements in matrix **T*** gives AE and AC features, respectively. Dualistic relationship between AE and AC can describe global behavior of expanding or contracting. For example, in Fig. 3d AC>AE shows trajectory has a global contracting behavior. In other words, AE/AC ratio can be defined as expanding ratio. After extracting global behavior of trajectory, AES and ACS present speed of this behavior. Average speed of expanding and contracting cannot describe global behavior. For example if according to AE/AC ratio, the trajectory has global contracting behavior, it is possible that AES>ACS. This conflict is caused by inequality of positive and negative element of matrix **T***. Trajectories in Fig. 3c and d look the same, but speed of moving through time of trajectory in Fig. 3d is greater than Fig. 3c, so AES_d is greater than AES_c. The trajectory in Fig. 3c is interpolated by the trajectory in Fig. 3d by a rate of 10, so $AES_d / AES_c \approx 10$.

Complexity feature is related to variations of speed of expansion and contraction of trajectory. Increasing variations of speed of expansion and contraction and subsequently increasing value of complexity feature means existence of more local behavioral diversity. Two trajectories must have the same number of state vectors to compare complexity feature. For example, trajectories in Fig. 3d and g and trajectories in Fig. 3c and h have the same number of state vectors, but according to Table 1 $Complexity_h > Complexity_c$ and $Complexity_g > Complexity_d$.Moreover, the trajectories in Fig. 3g and h have random behavior so their complexity must be greater than that of other trajectories. In addition, in the same number of state vectors, random behavior has greater value of complexity.

To remove the effect of range of state vectors values, all features can be divided by OS feature. That means all features except OS feature are independent of amplitude range. For example trajectory in Fig. 3i is achieved by scaling trajectory in Fig. 3d ten times and as Table 1 shows all features of these two trajectories except OS are equal. Nevertheless, in some applications this normalization may be harmful and therefore be ignored.

Fig. 4 shows five one-dimensional trajectories and the feature values of these trajectories are reported in Table 2. Trajectories a, b and d have the simplest behavior in one-dimensional phase space (fixed, linear and periodic behavior, respectively), and complexity feature of these trajectories is almost zero. On the other hand, random behaviors have greater complexity values. Trajectory c has expanding behavior through the time, so for these trajectories AE>AC. Trajectory a, b, d and e do not have expanding or contracting behavior, so AC=AE. The rest of the features are the same.

4. Evaluation and discussion

Two time series, Mackey–Glass and Lorenz, are utilized to evaluate the proposed features. Lorenz equations were proposed by Edward Norton Lorenz to develop a simplified mathematical model for atmospheric convection. This model consists of 3 equations as

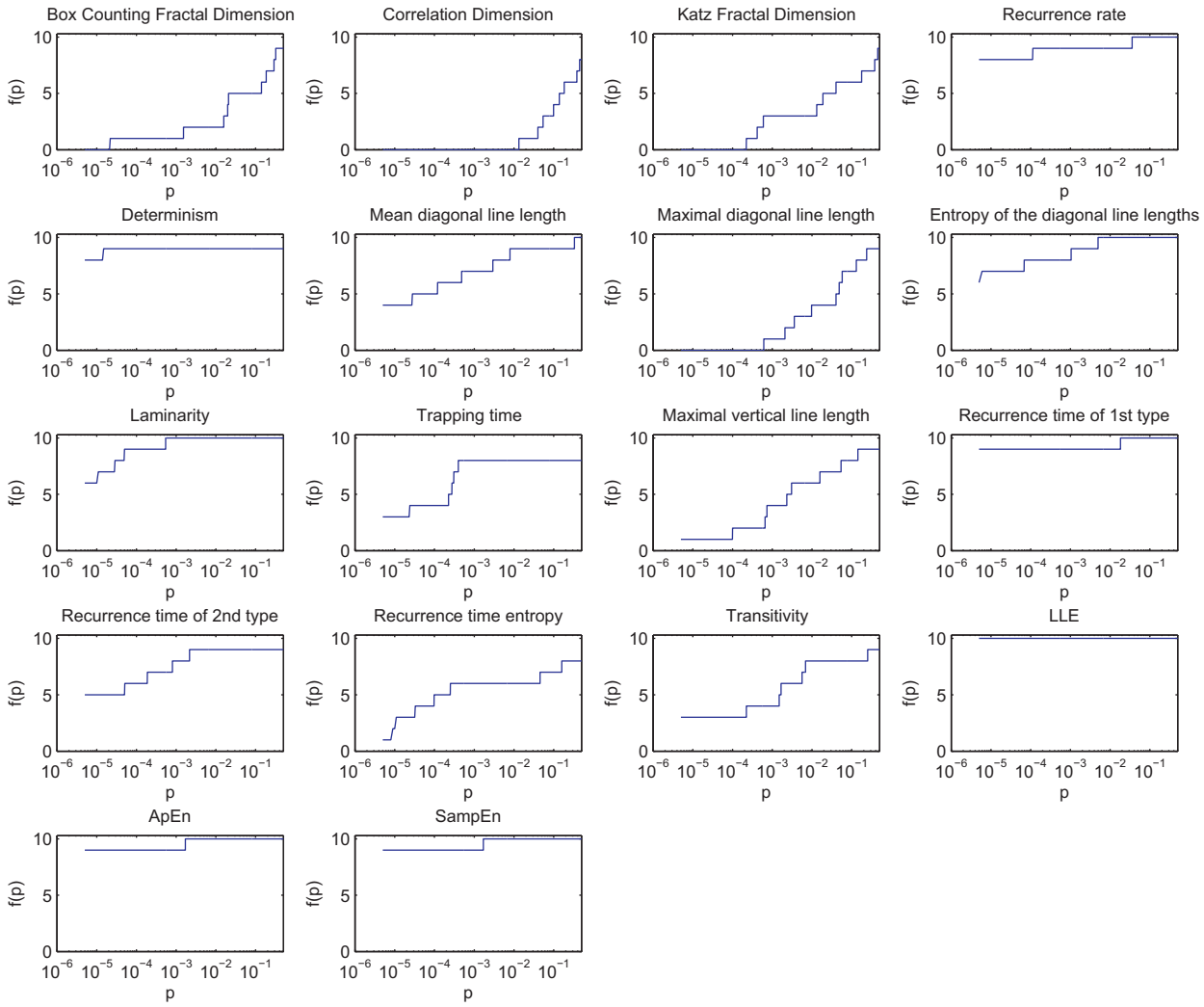

Fig. 13. The number of paired *t*-test between each common nonlinear feature of Lorenz signals with different parameters and random initial points whose p-values are less than specific value.

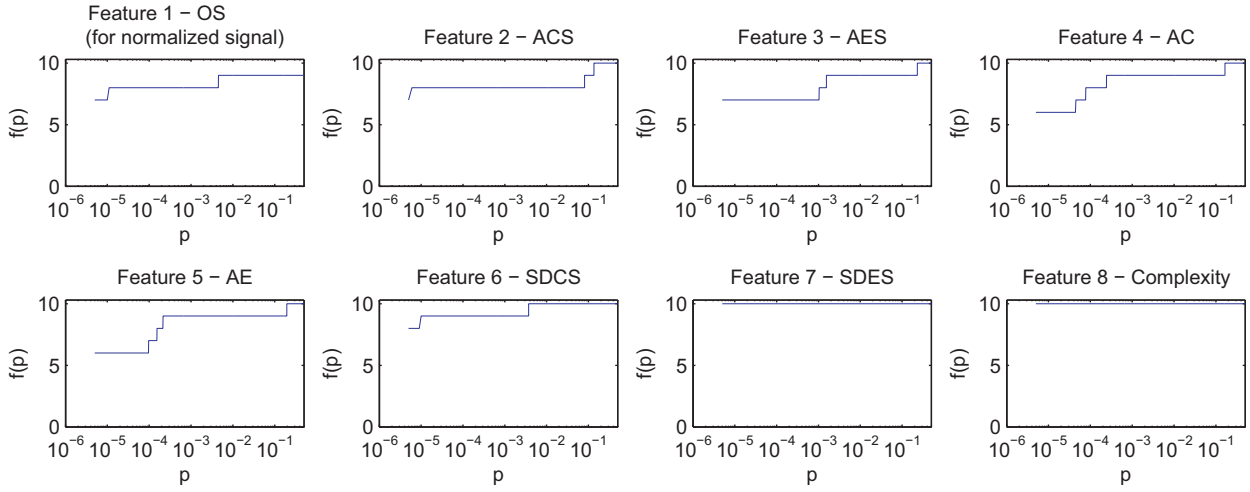

Fig. 14. The number of paired *t*-test between each volumetric feature of Lorenz signals with different parameters and random initial points whose p-values are less than specific value.

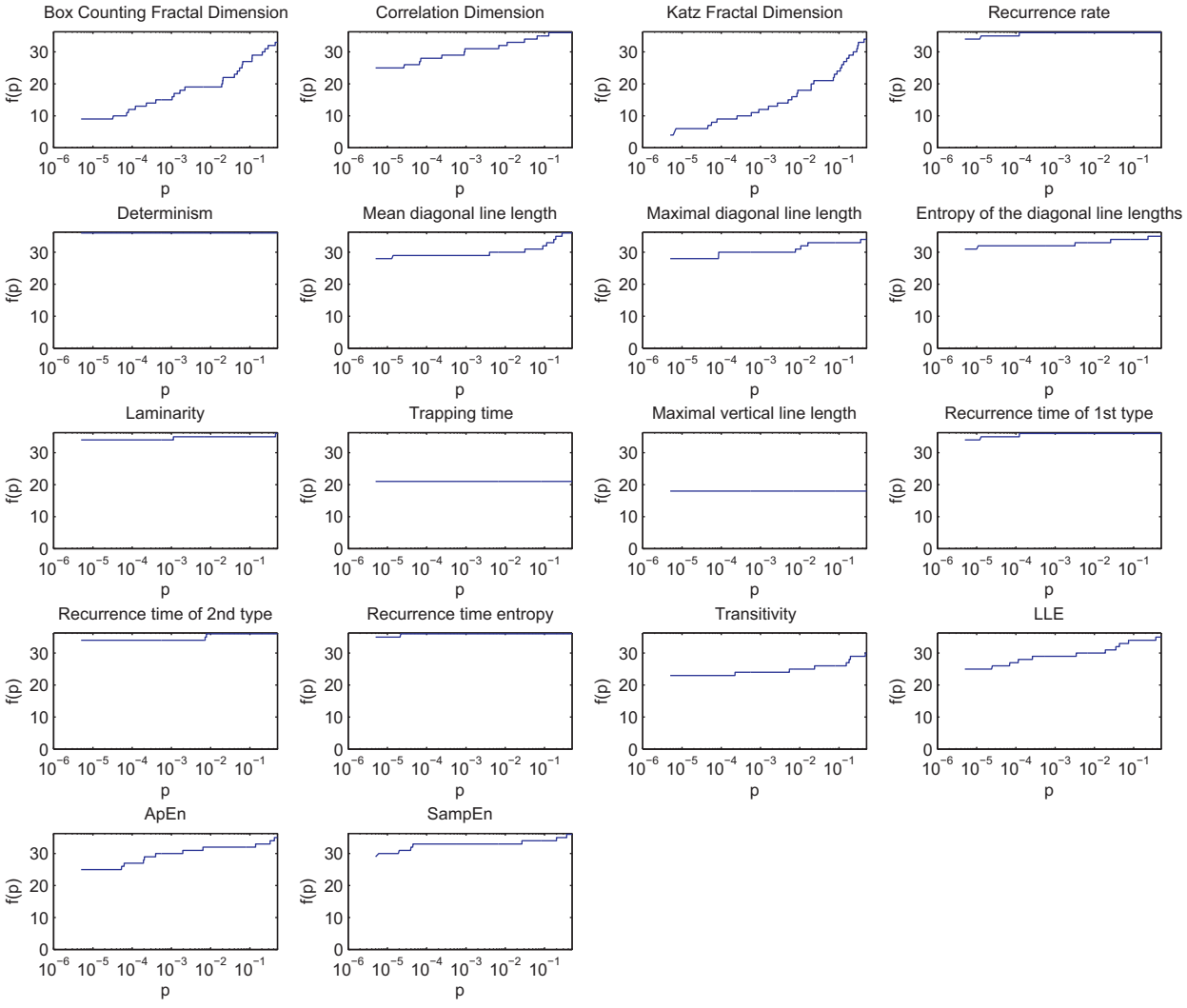

Fig. 15. The number of paired *t*-test between each common nonlinear feature of Mackey–Glass signals with different parameters and random initial points whose p-values are less than specific value.

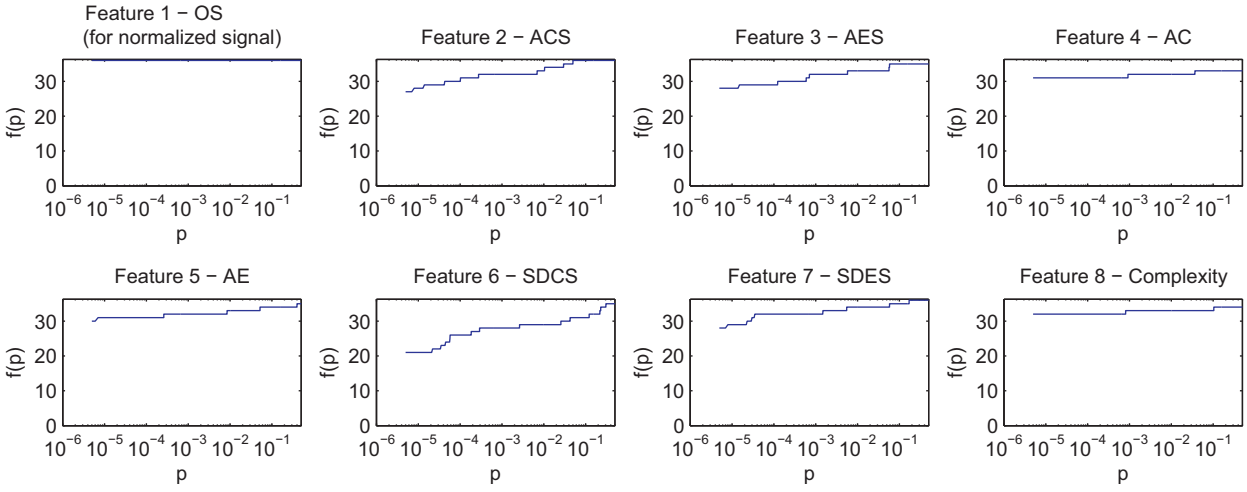

Fig. 16. The number of paired *t*-test between each volumetric feature of Mackey–Glass signals with different parameters and random initial points whose p-values are less than specific value.

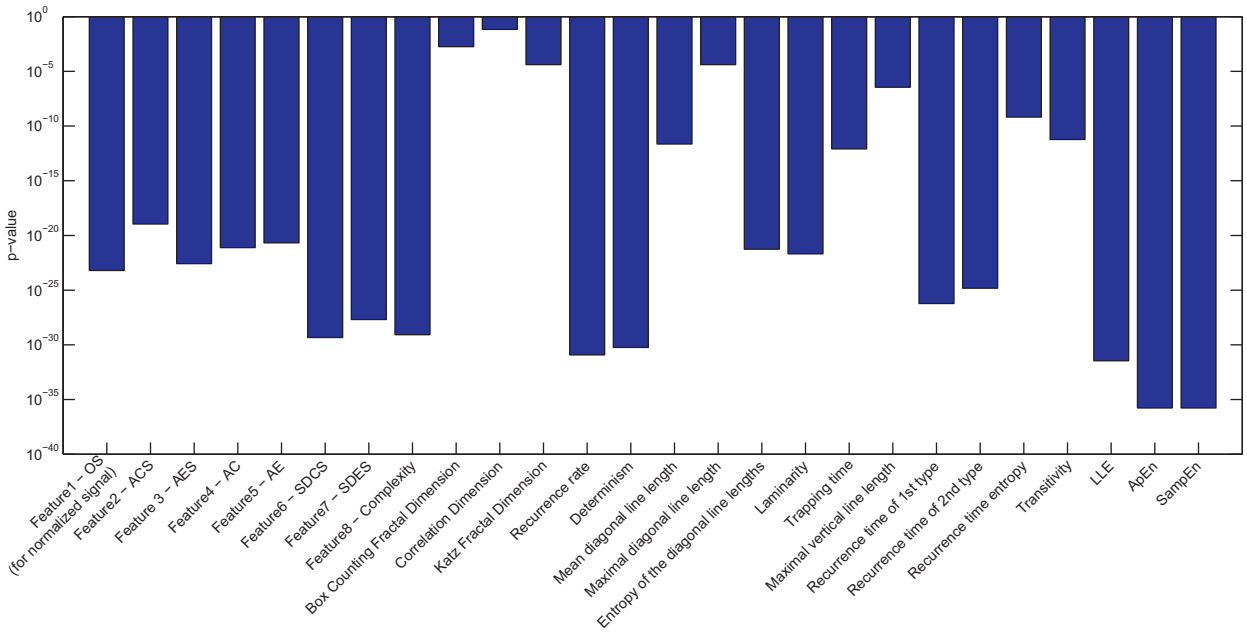

Fig. 17. P-value of ANOVA test for all volumetric and common nonlinear features for Lorenz signals with different parameters and random initial points.

Eq. (17).

$$\begin{aligned} \frac{dX}{dt} &= p(X-Y) \\ \frac{dY}{dt} &= XZ + rX - Y \\ \frac{dZ}{dt} &= XY - bZ \end{aligned} \tag{17}$$

Where, p, r and b are the parameters of the Lorenz model.

In this study only X value is used as time series. In simulation p and b are considered as constant parameters, $p = 16$ and $b = 4$. We aim at evaluating variations of the proposed features by changing r values (Fig. 5). The features are extracted from phase space. We embedded time series X to phase space by using Cao method with dimension $\mu = 3$ and delay $\tau = 6$. After embedding in $r = 10$, the trajectory is attracted to (-6,-6,-6) point (Fig. 6a). Therefore, the behavior of trajectory is compressing. For this trajectory with any initial point AC feature is greater that AE feature.

All the eight features are extracted for 4000 sample time series with $r = \{10, 20, 30, 40, 50,$ and $60\}$ and then different random initial points for 10 times. Fig. 7 shows box plot of the features of these trajectories.

As it can be seen in Fig. 6, by increasing r value the occupied space of trajectories increases. This behavior is characterized by increasing OS feature (Fig. 7a). Moreover, by increasing r value trajectories behave more complex and attractors become more complicated. In the proposed method, complexity is described as changes in local volumetric behavior. Therefore, by increasing complexity, SDES and SDCS features must be increased. Figs. 7f and g show increasing changes of local behavior (complexity in this context) by increasing r value. As can be seen, this features set makes the distinction between trajectories with different r values, although there are similarities between the trajectories with "$r = 40$ and 50" and "$r = 50$ and $r = 60$" (Fig. 6).

In this study, a discretized variant of the Mackey–Glass is used as nonlinear time series that can have chaotic behavior. Discretized variant of the Mackey–Glass is defined as:

$$X(i+1) = X(i) + \frac{aX(i-r)}{1 + X(i-r)^c} - bX(i) \tag{18}$$

where in this study $r = 17, b = 0.1$ and $c = 10$. "a" was considered as a variable parameter with values of $a = \{0.35, 0.4, 0.45, 0.5, 0.55, 0.6, 0.65, 0.7, 0.75\}$. An example of Mackey-Glass time series with random initialization is shown in Fig. 8.

These time series are very similar in time domain, by embedding with $\mu = 3$ and $\tau = 12$ parameters, their difference is shown in Fig. 9. The features set is extracted for 5000 sample time series with different a values and random initializations 10 times. Fig. 10 shows box plot of features of these trajectories. The features set is extracted for each time series making a complete distinction between time series with different a parameters.

4.1. Comparison with other nonlinear features

There are a number of common nonlinear features that are used in many different applications. Fractal dimensions, entropies, Lyapunov exponent and RQA features are the most commonly used nonlinear features. The ability of these features to distinguish between signals with different parameters and not to distinguish between chaotic signals with the same parameters and different initial points are compared with the proposed features. Two chaotic signals generators, Mackey–Glass and Lorenz, are used for this comparison. Figs. 11 and 12 show values of these nonlinear features that are extracted from Lorenz and Mackey–Glass signals 10 times for each parameters with random initial points.

Analysis of variance (ANOVA) test is employed to quantify ability of each feature to show the effect of changing parameters and initial points. ANOVA test can be used to analyze the differences among group means and their associated procedures. In most classification applications, the range of p-value is important and there is no significance in comparison with p-values, because only separability matters. In these applications p-values under specific numbers such as 0.05 are treated the same and mean the null hypothesis is rejected. However, in nonlinear and chaos quantification there are two important issues:

1. Separability by changing parameters. For example, vertical separability in boxes in Figs. 7 and 10–12.

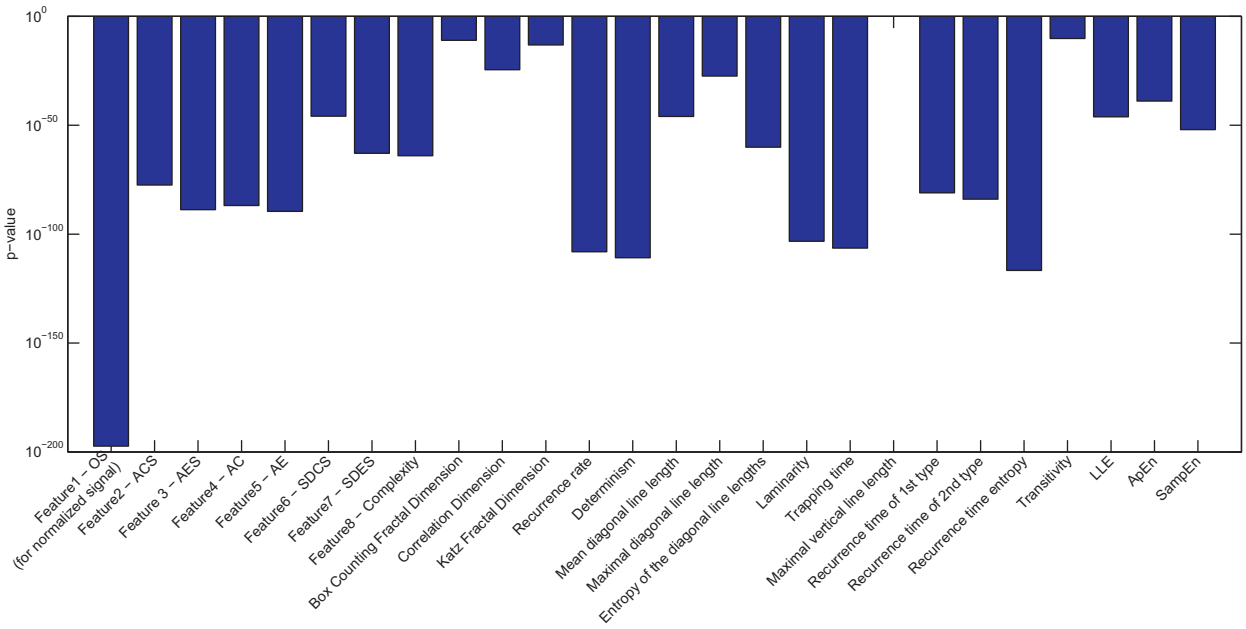

Fig. 18. P-value of ANOVA test for all volumetric and common nonlinear features for Mackey–Glass signals with different parameters and random initial points.

2. Inseparability by changing initial points with the same parameters. For example, lower height of each box in Figs. 7 and 10–12 with less variance is better.

With these issues, comparison of p-values is significant. Thus, to compare efficiency of features, p-value of ANOVA test and *t*-test can be used. Less p-value means more separability by changing parameters and fewer changes with different initial points with the same parameters. Two approaches are used for comparing p-values of common features and the method features. First, for each feature *t*-test's p-value of every pair of parameters is achieved and $f(p)$ (Eq. (19)) curves are plotted in Fig. 13–16.

$$f(p) = \textit{number of p-values of paired t-test that are less than p.} \tag{19}$$

The best feature is the one that has the most area under the $f(p)$ curve. Figs. 13 and 14 show that Complexity, SDES and LLE feature are the best in Lorenz signal quantification and Figs. 15 and 16 show that OS feature has the best performance as nonlinear quantification for Mackey–Glass signal.

In another approach, ANOVA test is applied on all features extracted from two signal sets. Figs. 17 and 18 show the p-value of tests. As it can be seen all volumetric features have less p-value than most of the other common nonlinear features.

5. Conclusion

In this paper, a volumetric behavior method that is an experimental and numerical approach has been proposed to characterize behavior of trajectories in phase space. This method extracts eight features from trajectories. The features are extracted from two matrices **T** and **T***. These matrixes are easily constructed and features extraction is done by simple operations, so the volumetric behavior method has very low complexity to extract the features.

Expanding and compressing behavior are identified by comparing AE and AC features. Also, the complexity of behavior is characterized by SDAE and SDAC features. Two nonlinear systems (Lorenz and Mackey–Glass) with variant parameters are evaluated to present the ability of the method to identify changes of systems. These eight features can be used to compare different time series of nonlinear systems and provide useful information about the trajectory of systems. This method requires to estimate embbeding dimension and time delay to reconstruct the phase space which may be challenging for some signals. Nevertheless, the proposed features are robust to initial conditions and sensitive to dynamic changes. Moreover, each of these features describes a specific and meaningful characteristic of trajectory in phase space.

The method should be employed in different areas of applications in the future work. As the objective can be different in different applications, some features may be more effective in those applications. In this case, metaheuristic algorithms such as monarch butterfly optimization (MBO) [31], earthworm optimization algorithm (EWA) [32], elephant herding optimization (EHO) [33] and moth search (MS) [34] algorithm can be used to select a good subset of features.

Acknowledgement

This study was supported by Cognitive Sciences and Technologies Council of Iran according to the contract No. 2688.

References

[1] Hilborn R. Chaos and nonlinear dynamics: an introduction for scientists and engineers. second ed. Oxford University Press; 2001.
[2] Mandelbrot B. How long is the coast of britain? statistical self-similarity and fractional dimension. Science 1967;156:636–8.
[3] Pincus S. Approximate entropy as a measure of system complexity. Proc Nation Acad Sci 1991;88:2297–301.
[4] Richman J, Moorman J. Physiological time-series analysis using approximate entropy and sample entropy. Am J Physiol Heart Circul Physiol 2000;278:2039–49.
[5] Goa J, Hu J, Tung W. Entropy measures for biological signal analyses. Nonlinear Dyn 2012;68:431–44.
[6] Pincus S, Gladstone I, Ehrenkranz R. A regularity statistic for medical data analysis. J Clin Monit Comput 1991;7:335–45.
[7] Sadri S, Wu C. Modified lyapunov exponent, new measure of dynamics. Nonlinear Dyn 2014;78:2731–50.
[8] Sagan H. Space-filling curves. Springer-Verlag, Berlin; 1994.
[9] Higuchi T. Approach to an irregular time series on the basis of the fractal theory. Physica D 1988;31:277–83.
[10] Katz M. Fractals and the analysis of waveforms. Comput Biol Med 1988;18:145–56.
[11] Faloutsos C, Ranganathan M, Manolopoulos Y. Fast subsequence matching in time-series databases. In: Proceedings of the ACM SIGMOD international conference on management of data; 1994. p. 419–29.

[12] Chan K, Fu A. Efficient time series matching by wavelets. In: Proceedings of the IEEE international conference on data engineering; 1999. p. 126–33.
[13] Ravi Kanth K, Agrawal D, Singh A. Dimensionality reduction for similarity searching in dynamic databases. In: Proceedings of the ACM SIGMOD international conference on management of data; 1998. p. 166–76.
[14] Liu K, Hu R-J, Cattani C, Xie G-N, Yang X-J, Zhao Y. Local fractionalz-transforms with applications to signals on cantor sets. Abstr Appl Anal 2014;2014:1–6. doi:10.1155/2014/638648.
[15] Yang X-J, Baleanu D, Srivastava HM, Machado JAT. On local fractional continuous wavelet transform. Abstr Appl Anal 2013;2013:1–5. doi:10.1155/2013/725416.
[16] Zhao Y, Baleanu D, Cattani C, Cheng D-F, Yang X-J. Local fractional discrete wavelet transform for solving signals on cantor sets. Math Probl Eng 2013;2013:1–6. doi:10.1155/2013/560932.
[17] Marwan N, Romano M, Thiel M, Kurths j. Recurrence plots for the analysis of complex systems. Phys Rep 2007;438:237–329.
[18] Eckmann J-P, Oliffson Kamphorst S, Ruelle D. Recurrence plots of dynamical systems. Europhys Lett 1987;4:973.
[19] Cullen J, Saleem A, Swindell R, Burt P, Moore C. Measurement of cardiac synchrony using approximate entropy applied to nuclear medicine scans. Biomed Sig Process Control 2010;5:32–6.
[20] Song Y, Crowcroft J, Zhang I. Automatic epileptic seizure detection in eegs based on optimized sample entropy and extreme learning machine. J Neurosci Methods 2012;210:132–46.
[21] Caesarendra W, Kosasih B, Tieu A, Moodie C. Application of the largest lyapunov exponent algorithm for feature extraction in low speed slew bearing condition monitoring. Mech Syst Sig Process 2015;50:116–38.
[22] Banerjee A, Pohit G. Crack investigation of rotating cantilever beam by fractal dimension analysis. Procedia Technol 2014;50:188–95.
[23] Gandhi A, Joshi J, Kulkarni A, Jayaraman V, B K. Svr-based prediction of point gas hold-up for bubble column reactor through recurrence quantification analysis of lda time-series. Int J Multiphase Flow 2008;34:1099–107.
[24] Ghafari S, Golnaraghi F, Ismail F. Effect of localized faults on chaotic vibration of rolling element bearings. Nonlinear Dyn 2008;53:287–301.
[25] Wang W, Wu Z, Chen J. Fault identification in rotating machinery using the correlation dimension and bispectra. Nonlinear Dyn 2001;25:383393.
[26] Nguyen S, Chelidze D. New invariant measures to track slow parameter drifts in fast dynamical systems. Nonlinear Dyn 2014;25.
[27] Packard N, Crutchfield J, Farmer J, Shaw R. Geometry from a time series. Phys Rev Lett 1980;45:712–15.
[28] Takens F, Crowcroft J, Zhang I. Detecting strange attractors in turbulence. Dyn Syst Turbul Lect Notes Math 1981;898:361–81.
[29] Kennel M, Brown R, Abarbanel H. Determining embedding dimension for phase-space reconstruction using a geometrical construction. Phys Rev A 1992;45:3403–11.
[30] Fraser A, Swinney H. Independent coordinates for strange attractors from mutual information. Phys Rev A 1986;33:1134–40.
[31] Wang G-G, Deb S, Cui Z. Monarch butterfly optimization. Neural Comput Appl 2015a. doi:10.1007/s00521-015-1923-y.
[32] Wang GG, Deb S, Coelho LDS. Earthworm optimization algorithm: a bio-inspired metaheuristic algorithm for global optimization problems. Int J Bio Inspired Comput 2015b;1(1):1. doi:10.1504/ijbic.2015.10004283.
[33] Wang G-G, Deb S, dos S Coelho L. Elephant herding optimization. 2015 3rd international symposium on computational and business intelligence (ISCBI). IEEE; 2015c. doi:10.1109/iscbi.2015.8.
[34] Wang G-G. Moth search algorithm: a bio-inspired metaheuristic algorithm for global optimization problems. Memetic Comput 2016. doi:10.1007/s12293-016-0212-3.